

DFT-spread-OFDM Based Chirp Transmission

Alphan Şahin, Nozhan Hosseini, Hosseinali Jamal, and David W. Matolak

Electrical Engineering Department, University of South Carolina, Columbia, SC, USA

Email: asahin@mailbox.sc.edu, nozhan@email.sc.edu, hjamal@email.sc.edu, matolak@cec.sc.edu

Abstract—In this study, we propose a low-complexity transceiver for chirp-based communications by exploiting discrete Fourier transform-spread orthogonal frequency division multiplexing (DFT-s-OFDM). We show that a well-designed frequency-domain spectral shaping (FDSS) function for DFT-s-OFDM can convert its single-carrier nature to a linear combination of chirp signals circularly translated in the time domain. By utilizing Bessel functions and Fresnel integrals for FDSS coefficients, we synthesize modulated sinusoidal and linear chirps. We show that the chirp signals with low ripples in the frequency domain result in a lower bit-error ratio (BER) due to the less noise enhancement during the single-tap frequency-domain equalization (FDE). Numerical results indicate that the signal-to-noise ratio (SNR) degradation can be as high as 4 dB for sinusoidal chirps while it is approximately 0.5 dB for linear chirps as compared to DFT-s-OFDM without FDSS. The proposed scheme offers a way to efficiently generate chirp signals that can be used in Internet-of-Things (IoT) or radar applications with existing DFT-s-OFDM transceivers.

I. INTRODUCTION

Chirp signals are prominent for radar and communication applications in the sense that they can sweep a large spectrum while still being constant-envelope signals, i.e., they provide a significant robustness against non-linear distortions. To provide a longer range and higher resolution for radar systems, chirps were first utilized by S. Darlington at Bell Labs [1]. Recently, there is a growing interest in their potential use in today’s major communication systems, e.g., 3GPP Fifth Generation (5G) New Radio (NR) and IEEE 802.11 Wi-Fi, to address some emerging applications such as short-range wireless sensing, simultaneous radar & communications, and Internet-of-Things (IoT). However, the physical layer of these communication systems are based on orthogonal frequency division multiplexing (OFDM). In this study, we aim at addressing the challenge of synthesizing chirp signals within an OFDM framework.

There is an extensive literature dealing with the chirp signals for communications. The idea of encoding bits as negative or positive slopes in time-frequency (TF) plane goes back to late 1950s, introduced by S. Darlington and M. R. Winkey. An initial experimental work for chirp modulation was discussed in [2] for long-range air/ground communications in the high-frequency (HF) band. Advances in electronics have accelerated the development of more sophisticated schemes. For example, the authors in [3] investigated an orthogonal amplitude-variant linear chirp set where each chirp has a different chirp rate. In [4], X. Ouyang and J. Zhao presented a way of constructing orthogonal chirps by introducing a term to the exponent of discrete Fourier transform (DFT) kernels. As the proposed

method in [4] translates the chirp signals in the frequency domain, the signal bandwidth increases with the number of chirps. To limit the bandwidth, the authors proposed additional up-sampling and filtering at baseband, which folds the chirps in the frequency domain. The Fresnel transform and fractional Fourier transform (FrFT) were adopted to generate orthogonal chirp sets in [4] and [5], respectively. In [6], binary chirp spread spectrum (BCSS) signaling in quasi-synchronous transmission were investigated by analyzing performance in a multi-user scenario. Two non-linear chirps were proposed to improve the bit-error ratio (BER) performance. Furthermore, the BER performance of quartic and linear chirps was compared in an empirical aeronautical channel model. The authors in [7] and [8] proposed an iterative receiver to improve the BER performance under frequency-selective fading channels and investigated space-time coding schemes for orthogonal chirps. In addition, a proprietary chirp spread spectrum (CSS) modulation, called Long Range (LoRa), was introduced by Samtec for IoT applications. The chirps for short-range wireless sensing was also brought up in IEEE 802.11 Wi-Fi meetings, e.g., [9].

To best of our knowledge, the available methods in the literature do not construct chirp signals within an OFDM framework. To address this issue, we present a method to generate chirp signals based on discrete Fourier transform-spread orthogonal frequency division multiplexing (DFT-s-OFDM) adopted in 3GPP 5G NR and 3GPP Long-Term Evolution (LTE) (see [10]–[12] and the references therein). The proposed method relies on the design of frequency-domain spectral shaping (FDSS) function applied after DFT spreading to convert the single-carrier pulses, i.e., Dirichlet sinc functions [11], to a set of chirp signals translated uniformly in time. The proposed method limits the bandwidth of the chirp signals without additional operations mentioned in [4]. As the chirp signals are generated within the given a number of subcarrier bins by point-to-point multiplications, it also allows existing DFT-s-OFDM transceiver to modulate and demodulate chirp signals while supporting multiple users.

II. PROPOSED SCHEME

For the proposed scheme, we transmit the data symbols over the basis functions $\{B_{\tau_0}(t), B_{\tau_1}(t), \dots, B_{\tau_{M-1}}(t)\}$ constructed by translating a chirp signal circularly in time, where τ_m is the amount of circular shift. We assume that the shifts in time are uniformly spaced between 0 and T_s , i.e., $\tau_m = m/M \times T_s$,

where T_s is the chirp duration. The complex baseband signal $p(t)$ can then be expressed as

$$p(t) = \sum_{m=0}^{M-1} d_m B_{\tau_m}(t) = \sum_{m=0}^{M-1} d_m e^{j\psi_m(t)}, \quad (1)$$

where $d_m \in \mathbb{C}$ is the m th modulation or a pilot symbol and $\psi_m(t)$ is the phase of the carrier for the m th basis function. Therefore, the instantaneous frequency of the m th chirp signal $B_{\tau_m}(t)$ around the carrier frequency f_c can be obtained as $F_m(t) = \frac{1}{2\pi} d\psi_m(t)/dt$ Hz. The waveform given in (1) is a simple linear combination of the basis functions related to chirp signals. However, it is implicitly related to DFT-s-OFDM. This relation can be shown as follows:

Let $B_{\tau_m}(t) = e^{j\psi_m(t)}$ be an arbitrary band-limited function with the period of T_s . Hence, it can be expressed as

$$e^{j\psi_m(t)} = \sum_{k=-\infty}^{\infty} c_k e^{j2\pi k \frac{t-\tau_m}{T_s}}, \quad (2)$$

where c_k is the k th Fourier coefficient given by

$$c_k = \frac{1}{T_s} \int_{T_s} e^{j\psi_0(t)} e^{-j2\pi k \frac{t}{T_s}} dt. \quad (3)$$

By using (2) and $\tau_m = m/M \times T_s$, (1) can be expressed as

$$\begin{aligned} p(t) &= \sum_{m=0}^{M-1} d_m \sum_{k=-\infty}^{\infty} c_k e^{j2\pi k \frac{t-\tau_m}{T_s}} \\ &\approx \sum_{k=L_d}^{L_u} c_k \sum_{m=0}^{M-1} d_m e^{-j2\pi k \frac{m}{M}} e^{j2\pi k \frac{t}{T_s}}, \end{aligned} \quad (4)$$

where $L_d < 0$ and $L_u > 0$ are integer values. The approximation is due to the fact that $B_{\tau_m}(t)$ is a band-limited function, i.e., c_k is a decaying Hermitian symmetric function as k goes to positive or negative infinity. Finally, by sampling $p(t)$ with the period T_s/N , the discrete-time signal can be obtained as

$$p\left(\frac{nT_s}{N}\right) \approx \underbrace{\sum_{k=L_d}^{L_u} c_k \underbrace{\sum_{m=0}^{M-1} d_m e^{-j2\pi k \frac{m}{M}}}_{\text{M-point DFT}} e^{j2\pi k \frac{n}{N}}}_{\text{Frequency-domain spectral shaping}}. \quad (5)$$

In other words, (1) is a special DFT-s-OFDM symbol that can be implemented by 1) calculating the M -point DFT of a data vector, i.e., $[d_0, d_1, \dots, d_{M-1}]$, 2) multiplying each element of the output of DFT with the corresponding Fourier coefficient, i.e., FDSS or windowing in frequency, and 3) calculating the N -point inverse DFT (IDFT) of the shaped sequence after padding it with $N - (L_u - L_d + 1)$ zero symbols (i.e., guard subcarriers in OFDM). In this study, without loss of generality, we assume $L_u - L_d + 1 = M$ to ensure that the FDSS occurs within the bandwidth spanned by M subcarriers. Therefore, the chirp bandwidth should be less than or equal to M/T_s .

Note that FDSS was discussed in 3GPP LTE and 3GPP 5G NR uplink as an implementation-specific option to reduce

peak-to-average-power ratio (PAPR) further for DFT-s-OFDM. Based on (5), we show the same DFT-s-OFDM transmitter can also generate arbitrary chirp signals by choosing the shaping coefficients properly without compromising the other features of the physical layer design in these communication systems. As compared to the method in [4], it does not cause any bandwidth expansion as the chirps are circularly shifted versions of each other in the time domain while eliminating additional processing to avoid aliases.

A. Sinusoidal Chirps

Let the instantaneous frequency of $B_{\tau_0}(t)$ around the carrier frequency f_c be a sinusoidal function given by $F_0(t) = \frac{D}{2T_s} \cos\left(2\pi \frac{t}{T_s}\right)$. Therefore, $\psi_0(t) = \frac{D}{2} \sin\left(2\pi \frac{t}{T_s}\right)$. It is well-known that $e^{j\psi_0(t)}$ can be decomposed as

$$e^{j\frac{D}{2} \sin\left(2\pi \frac{t}{T_s}\right)} = \sum_{k=-\infty}^{\infty} J_k\left(\frac{D}{2}\right) e^{j2\pi k \frac{t}{T_s}}, \quad (6)$$

where $J_k(\cdot)$ is the Bessel function of the first kind of order k . Hence, c_k is equal to $J_k\left(\frac{D}{2}\right)$ for sinusoidal chirps. The maximum frequency deviation of each basis function and the effective bandwidth of the transmitted signal $p(t)$ are equal to $\Delta f = D/2T_s$ Hz and D/T_s Hz, respectively. Therefore, $D \leq M$ must hold true to form the sinusoidal chirp in (5).

B. Linear Chirps

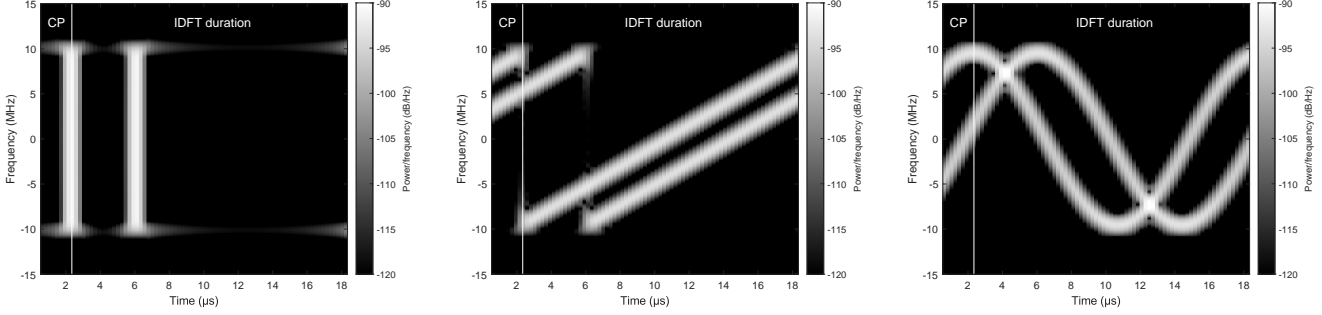
Assume that the instantaneous frequency of $B_{\tau_0}(t)$ around the carrier frequency f_c changes from $-\frac{D}{2T_s}$ Hz to $\frac{D}{2T_s}$ Hz, i.e., $F_0(t) = \frac{D}{2T_s} \left(\frac{2t}{T_s} - 1\right)$, which results in $\psi_0(t) = \frac{\pi D}{T_s} \left(\frac{t^2}{T_s} - t\right)$. The shaping coefficients c_k can be obtained as

$$c_k = \sqrt{\frac{\pi}{D}} e^{-j\frac{(2\pi k)^2}{2D} - j\pi k} (C(x_1) + C(x_2) + jS(x_1) + jS(x_2)), \quad (7)$$

where $C(\cdot)$ and $S(\cdot)$ are the Fresnel integrals with cosine and sine functions, respectively, and $x_1 = (D/2 + 2\pi k)/\sqrt{\pi D}$ and $x_2 = (D/2 - 2\pi k)/\sqrt{\pi D}$. Similar to the sinusoidal chirp, the condition $D \leq M$ must be satisfied to form the linear chirp.

C. Receiver

The receiver for the proposed scheme is similar to a typical DFT-s-OFDM receiver. After the cyclic prefix (CP) is discarded, the DFT of the received signal is calculated. In the frequency domain, the impact of channel is removed with a single-tap minimum mean square error (MMSE)-frequency-domain equalization (FDE). The modulation symbols are obtained after an M -IDFT operation on the equalized signal vector. For a practical receiver, the shaping coefficients can be considered as part of the channel frequency response and estimated through channel estimation procedure. From this aspect, the proposed scheme does not require any change from a practical DFT-s-OFDM receiver. On the other hand, if the shaping coefficients are available at the receiver *a priori*, the receiver can perform better as they do not need to be estimated.



(a) Two pulses (plain DFT-s-OFDM).

(b) Two linear chirps with DFT-s-OFDM.

(c) Two sinusoidal chirps with DFT-s-OFDM.

Figure 1. Spectrogram of the signals generated with DFT-s-OFDM for only two active symbols (i.e., d_0 , d_{75}).

III. NUMERICAL RESULTS

For computer simulations, we consider an OFDM framework where the symbol duration $T_s = 16.67 \mu\text{s}$, i.e., the subcarrier spacing is 60 kHz. The CP duration is set to 2.34 μs . We assume that the transmitter exploits $M = 336$ subcarriers, i.e., the bandwidth is 20.16 MHz. For the linear and sinusoidal chirps, we choose $D = 318$ to not distort chirp signals due to the truncation in frequency. We generate the data symbols based on quadrature phase shift keying (QPSK) modulation and use $M = 336$ basis functions simultaneously unless otherwise stated. The multi-path channel is generated based on Extended Vehicular A (EVA) power delay profile. For the channel coding, IEEE 802.11ay low-density parity check (LDPC) code with the rate of 1/2 is employed where the codeword length is 672.

In Figure 1, we provide spectrograms for plain DFT-s-OFDM (i.e., no FDSS), linear chirps, and sinusoidal chirps when only d_0 and d_{75} are set to 1. Since plain DFT-s-OFDM is a form of single carrier waveform, the symbols d_0 and d_{75} appear as two pulses in time as in Figure 1(a). In contrast, the same symbols result in two linear and sinusoidal chirps transmitted in simultaneously as given in Figure 1(b) and Figure 1(c), respectively. We also observe that there is a sudden frequency change for linear chirps. On the other hand, the abrupt instantaneous frequency changes are avoided for the sinusoidal chirps. This is due to the fact that sinusoidal chirp is a continuous periodic function while linear chirp is a discontinuous periodic function in (2).

In Figure 2, the amplitude of the shaping coefficients are given for the linear and sinusoidal chirp signals. The chirp signals do not distribute symbol energy to the subcarriers evenly. While the amplitude variation for linear chirp signals are relatively mild except the edge subcarrier, they can be large for sinusoidal chirps. A large amplitude variation can lead to two issues: ripples in the spectrum and noise enhancement. As shown in Figure 3, the main lobe of the spectrum is not flat for linear and sinusoidal chirps. Particularly, a majority of the symbol energy is carried over the edge subcarrier bins for sinusoidal chirps. Secondly, large ripples affect the BER performance. For example, the amplitude of the shaping coefficients can be very small values for sinusoidal chirps.

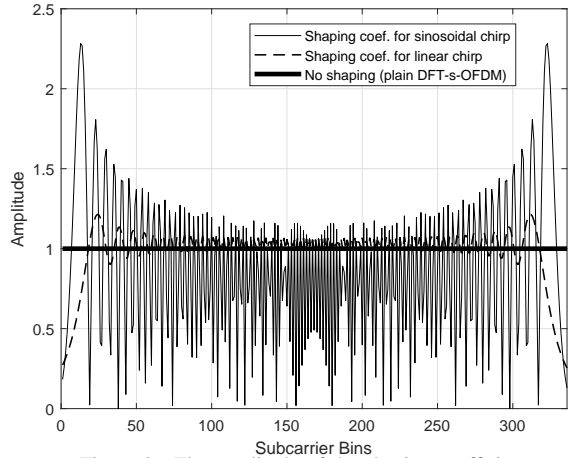


Figure 2. The amplitude of the shaping coefficients.

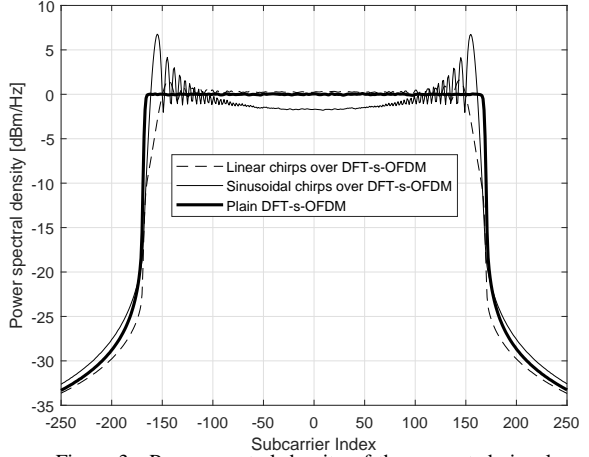


Figure 3. Power spectral density of the generated signals.

Therefore, the corresponding bins are more prone to noise as compared to the other bins with large shaping coefficients.

In Figure 4, we compare PAPR distributions. The introduction of FDSS for generating chirp signals does not keep the low PAPR benefit of DFT-s-OFDM. This result is expected as the symbol energy is distributed in both time and frequency for the chirp signals. When multiple chirp signals are transmitted in parallel, the chirp signals can constructively or destructively add up, which increases the PAPR.

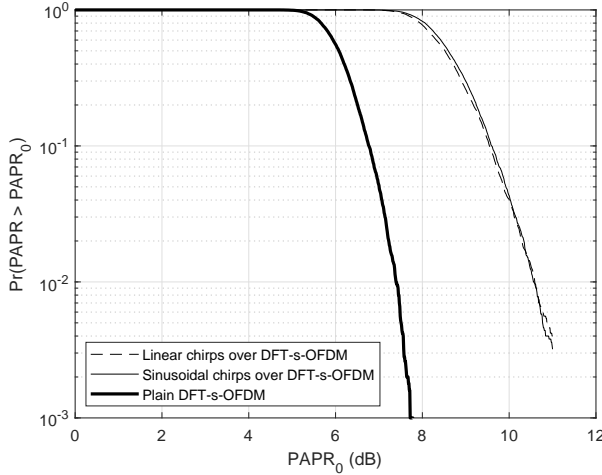


Figure 4. PAPR distribution.

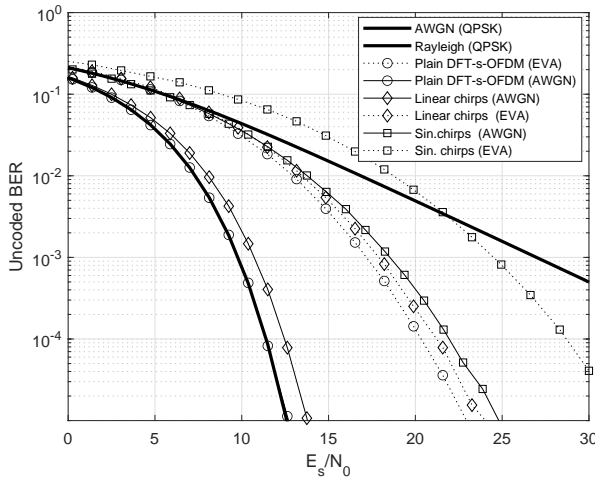


Figure 5. BER (uncoded) performance.

In Figure 5 and Figure 6, uncoded BER and coded BER curves are provided for additive white Gaussian noise (AWGN) and multi-path fading channels. For uncoded bits, we observe a large degradation for the sinusoidal chirps in both AWGN and multipath channels, as compared to DFT-s-OFDM. However, the difference between linear chirps and DFT-s-OFDM is approximately 1 dB for uncoded bits. When the channel encoder is introduced, the degradation reduces to approximately 0.5 dB while it is approximately 4 dB for the sinusoidal chirps in AWGN and multi-path fading channels. Thus, linear chirps provide more reliable links as compared to sinusoidal chirps for this particular design.

IV. CONCLUDING REMARKS

In this study, we show that chirp signals can be generated with DFT-s-OFDM via well-designed shaping coefficients. The main benefit of the proposed approach is that a typical DFT-s-OFDM receiver with a single-tap FDE-MMSE can decode the modulated chirps. The numerical results show that the amplitude variations in the shaping coefficients adversely

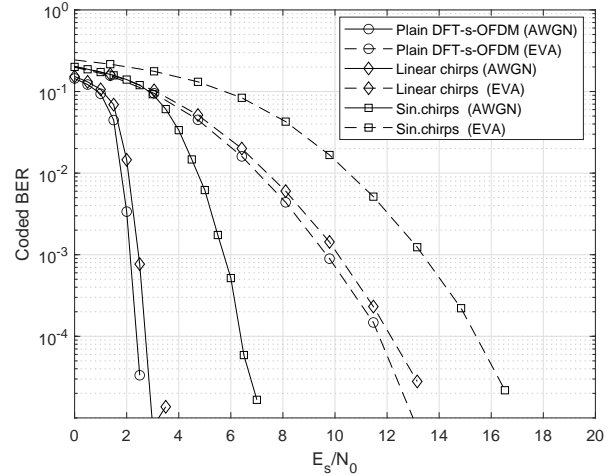


Figure 6. BER (coded) performance (LDPC).

affect the BER performance due to the noise enhancement during equalization. While the signal-to-noise ratio (SNR) degradation is approximately 0.5 dB for linear chirps, it reaches 4 dB for the sinusoidal chirps due to the large variations, as compared to DFT-s-OFDM without any FDSS. The proposed approach provides insight into how the waveform for radar & communications and IoT applications can be synthesized without introducing major modifications to the physical layer of today's wireless communication standards.

REFERENCES

- [1] S. Darlington, "Pulse transmission," Patent US2 678 997A, Dec., 1949.
- [2] G. F. Gott and J. P. Newsome, "H.F. data transmission using chirp signals," *Proceedings of the Institution of Electrical Engineers*, vol. 118, no. 9, pp. 1162-1166, Sep. 1971.
- [3] Hao Shen and A. Papandreou-Suppappola, "Diversity and channel estimation using time-varying signals and time-frequency techniques," *IEEE Trans. Signal Process.*, vol. 54, no. 9, pp. 3400-3413, Sep. 2006.
- [4] X. Ouyang and J. Zhao, "Orthogonal chirp division multiplexing," *IEEE Trans. Commun.*, vol. 64, no. 9, pp. 3946-3957, Sep. 2016.
- [5] Y. Ju and B. Barkat, "A new efficient chirp modulation technique for multi-user access communications systems," in *Proc. IEEE International Conference on Acoustics, Speech, and Signal Processing*, vol. 4, May 2004, pp. iv-937.
- [6] N. Hosseini and D. W. Matolak, "Nonlinear quasi-synchronous multi user chirp spread spectrum signaling," *CoRR*, vol. abs/1909.04143, 2019.
- [7] R. Bomfin, M. Chafii, and G. Fettweis, "Low-complexity iterative receiver for orthogonal chirp division multiplexing," in *Proc. IEEE Wireless Communications and Networking Conference Workshop (WCNCW)*, April 2019, pp. 1-6.
- [8] ———, "Performance assessment of orthogonal chirp division multiplexing in MIMO space time coding," in *Proc. IEEE 5G World Forum (5GWF)*, Sep. 2019, pp. 220-225.
- [9] T. X. Han and et. al., "Wi-Fi sensing – follow up," IEEE 802.11-19/1500, 2019.
- [10] H. Sari, G. Karam, and I. Jeanclaude, "Transmission techniques for digital terrestrial TV broadcasting," *IEEE Commun. Mag.*, vol. 33, no. 2, pp. 100-109, Feb. 1995.
- [11] A. Sahin, R. Yang, E. Bala, M. C. Beluri, and R. L. Olesen, "Flexible DFT-S-OFDM: Solutions and challenges," *IEEE Commun. Mag.*, vol. 54, no. 11, pp. 106-112, Nov. 2016.
- [12] "3rd Generation Partnership Project; Technical Specification Group Radio Access Network; NR physical layer; General description (Release 15)," *3GPP TS 38.201 V15.0.0*, pp. 1-12, Dec. 2017.